JOURNAL OF NANO- AND ELECTRONIC PHYSICS
Vol. **9** No 5, 05012(8pp) (2017)

ЖУРНАЛ НАНО- ТА ЕЛЕКТРОННОЇ ФІЗИКИ
Том **9** № 5, 05012(8cc) (2017)

Theory of Interband Optical Absorption in Quantum Wells Based on Bulk Materials with Anisotropic Nonparabolic Bands

V.V. Ivchenko[1,*], V.S. Shcherbiuk[2]

[1] *Kherson State Maritime Academy, 20, Ushakova Prosp., 73000 Kherson, Ukraine*
[2] *Kherson State University, 27, Universitetskaya Str., 73000 Kherson, Ukraine*

(Received 11 July 2017; revised manuscript received 18 August 2017; published online 16 October 2017)

Theory of interband optical absorption in rectangular quantum well with infinite barriers based on materials with strong nonparabolicity and anisotropy of energy spectra is developed. The numerical calculations for three-dimensional Dirac cadmium arsenide are done. Special attention is paid to the investigation of the effects of energy gap oscillation and "blue shift delay" in this material.

Keywords: Interband optical absorption, Quantum well, Cadmium arsenide, Energy gap oscillation, "Blue shift delay".

DOI: 10.21272/jnep.9(5).05012 PACS numbers: 73.21.Fg, 78.67.De

1. INTRODUCTION

Research of optical absorption in quantum wells (QWs) has led to the development of several practical devices, such as the quantum well infrared photodetector and the quantum cascade laser. In this area optical properties of wide range of two-dimensional systems were investigated both theoretically and experimentally (see e.g. [1] and references therein).

The importance of nonparabolicity bands influence on the selection rules and the oscillator strength in QW is shown in [2, 3] and in several other works. However, there are many semiconductors (narrow-gap II-V and one-axis strained III-V materials, chalcopyrite semiconductors, etc.), which are characterized not only by strong nonparabolicity of energy spectra but also energy dependent anisotropy of electron and holes energy bands due to the one axis symmetry of these crystals.

In this paper we construct theory of optical absorption in rectangular QWs with infinite barriers based on such materials. For this purpose we use modified version of the eight-band Kane model (so-called quasi-cubic approximation) [4] that is well proven itself in describing of electronic properties of these types of semiconductors. The numerical calculations are done for cadmium arsenide (Cd_3As_2) that is the three-dimensional Dirac semimetal with unique properties [5]. For example, this tetragonal crystal of the II-V family has large mobility, low effective mass and highly nonparabolic conduction band. It exhibits an inverted band structure (optical energy gap $\varepsilon_g < 0$) like HgTe. The interest to the low dimensional structures of this material is caused by recent realization of an ultrafast broadband QW photodetector based on Cd_3As_2 [6].

According to [7] the energy band structure of bulk Cd_3As_2 near the Brillouin zone center is depicted in Fig. 1. They are four relevant to the optical absorption edge twofold degenerate bands (we have omitted small k-dependent spin splitting of bands): conduction I band; heavy-hole (*hh*) valence band split off the light-hole (*lh*) valence band at $k = 0$ due to the tetragonal field splitting and spin-orbit (*so*) valence band splits off these last two bands at $k = 0$. Fig. 1a indicates that conduction and heavy-hole valence bands come into contact only at two (with $k_x = k_y = 0$) equal in modulus k_z points and the thermal energy gap becomes zero at this points. Moreover, the dispersion law for this pair of bands in the vicinity of these points is linear in k_z. Therefore, one can conclude that these two points are the Dirac points [8]. There is a "dent" in heavy-hole valence band between these points due to the exchange of curvature between it and the conduction band. There are the electronic states in this "dent". When the direction of wave vector $\mathbf{k}$ changes from k_z to $k_x(k_y)$ the shape of all dispersion curves changes also and the small energy gap between conduction and heavy-hole valence bands appears (Fig. 1 b). All these effects are caused by the negative value of ε_g (optical energy gap between conduction and light-hole valence bands that appears at the Γ-point) and non-zero value of δ (crystal field splitting parameter).

2. THEORETICAL CALCULATIONS

The electronic wave function of our problem in the envelope function approximation (EFA) [9] can be chosen in such a form [10]:

$$\mathbf{\Psi(r)} = \begin{pmatrix} \Psi\uparrow \\ \Psi\downarrow \end{pmatrix} = \frac{1}{\sqrt{N}} \begin{pmatrix} F_1 S + F_3 Z + F_6 R_- + F_8 R_+ \\ F_2 S + F_4 Z - F_5 R_+ + F_7 R_- \end{pmatrix},$$

where N is a number of unit cells in crystal, $R_\pm = (X \pm iY)/\sqrt{2}$ and symbols $\uparrow$ and $\downarrow$ mean the spin-up and spin-down functions, respectively. S, X, Y, Z are the periodic Bloch amplitudes transformed as atomic s- and p- functions under the operations of the tetrahedral group at Γ-point. F_i are

* reterty@gmail.com

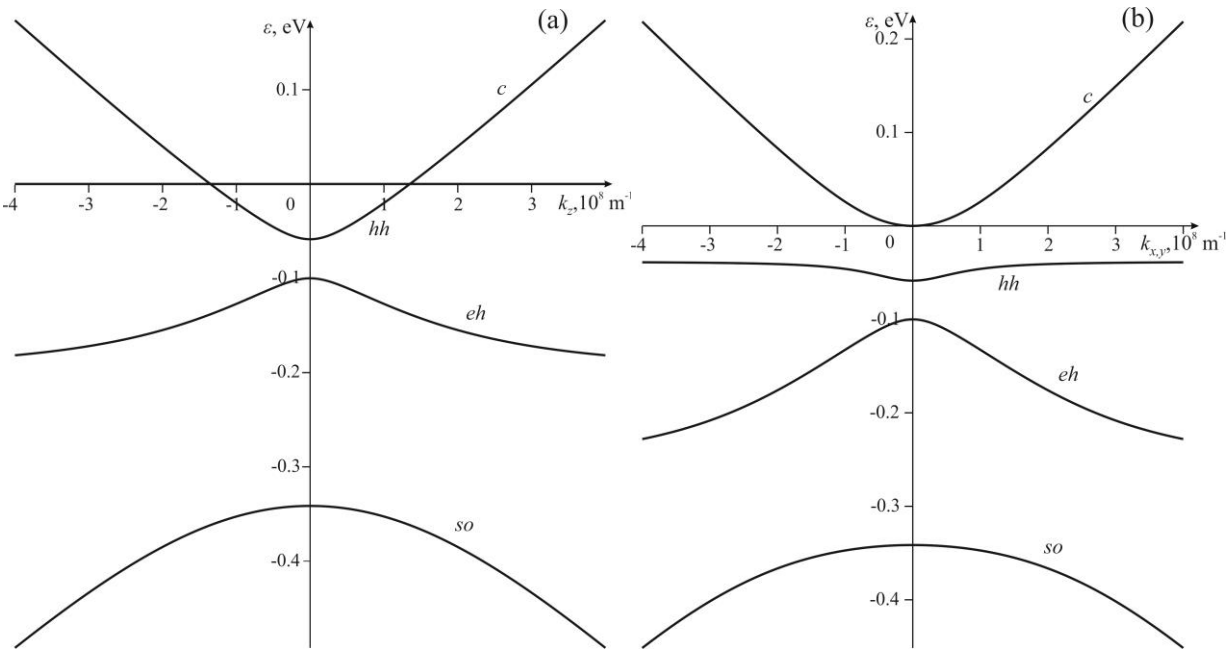

Fig. 1 – Structure of Cd_3As_2 conduction and valence bands near $\mathbf{k}$ =0. The wave vector is: a) parallel to the main crystalline z -axis; b) perpendicular to the main crystalline z -axis

envelope functions satisfying the set of eight coupled differential equations, which in the case of quasi-cubic approximation in the first order perturbation theory can be represented in the following matrix form [10]:

$$\begin{pmatrix} \varepsilon_1 & 0 & iP\hat{k}_z & 0 & 0 & iP\hat{k}_- & 0 & iP\hat{k}_+ \\ 0 & \varepsilon_1 & 0 & iP\hat{k}_z & -iP\hat{k}_+ & 0 & iP\hat{k}_- & 0 \\ -iP\hat{k}_z & 0 & \varepsilon_2 & 0 & \Delta_2 & 0 & 0 & 0 \\ 0 & -iP\hat{k}_z & 0 & \varepsilon_2 & 0 & \Delta_2 & 0 & 0 \\ 0 & iP\hat{k}_- & \Delta_2 & 0 & \varepsilon_3 & 0 & 0 & 0 \\ -iP\hat{k}_+ & 0 & 0 & \Delta_2 & 0 & \varepsilon_3 & 0 & 0 \\ 0 & -iP\hat{k}_+ & 0 & 0 & 0 & 0 & -\varepsilon & 0 \\ -iP\hat{k}_- & 0 & 0 & 0 & 0 & 0 & 0 & -\varepsilon \end{pmatrix} \begin{pmatrix} F_1 \\ F_2 \\ F_3 \\ F_4 \\ F_5 \\ F_6 \\ F_7 \\ F_8 \end{pmatrix} = 0 . \qquad (1)$$

Here $\varepsilon_1 = \varepsilon_g - \varepsilon$, $\varepsilon_2 = -(\varepsilon + \delta + \Delta/3)$, $\varepsilon_3 = -(\varepsilon + 2\Delta/3)$, $\Delta_1 = \sqrt{2}\Delta/3$, $\hat{k}_\pm = \left(1/\sqrt{2}\right)\left(\hat{k}_x \pm i\hat{k}_y\right)$, $\hat{k}_x, \hat{k}_y, \hat{k}_z$ are the components of the operator $\hat{\mathbf{k}} = -i\nabla$ Thus, the model along with ε_g and δ parameters requires knowledge of the values of spin-orbit splitting of valence band Δ and interband momentum matrix element P.

Let us express $F_3 \ldots F_8$ in terms of F_1, F_2 and eliminate them by substituting in the first two equations of the set (1). Then we obtain two equivalent differential equations for F_1 and F_2:

$$\left(\gamma(\varepsilon) + f_1(\varepsilon)\left(\frac{\partial^2}{\partial x^2} + \frac{\partial^2}{\partial y^2}\right) + f_2(\varepsilon)\frac{\partial^2}{\partial z^2}\right) F_{1,2} = 0, \qquad (2)$$

where

$$\gamma(\varepsilon) = \varepsilon\left[\left(\varepsilon - \varepsilon_g\right)\left(\varepsilon\left(\varepsilon + \Delta\right) + \delta\left(\varepsilon + \frac{2}{3}\Delta\right)\right)\right],$$

$$f_1(\varepsilon) = P^2\left[\varepsilon\left(\varepsilon + \frac{2}{3}\Delta\right) + \delta\left(\varepsilon + \frac{1}{3}\Delta\right)\right],$$

$$f_2(\varepsilon) = P^2\left[\varepsilon\left(\varepsilon + \frac{2}{3}\Delta\right)\right].$$

Let the main crystalline z -axis is perpendicular to the two-dimensional layer's plane. Then functions $F_{1,2}$ can be represented in form:

$$F_{1,2} = A_{1,2}\exp\left[i(k_x x + k_y y)\right]\Phi_{1,2}(z), \qquad (3)$$

where $A_{1,2}$ are the normalization constants; k_x, k_y are the components of two-dimensional wave vector $\mathbf{k}_\perp$ with modulus $k_\perp = \sqrt{k_x^2 + k_y^2}$, which characterizes electronic motion in the interface plane. Substituting right hand side of the equality (3) into the equation (2) we obtain:

$$A_{1,2} = -f_2\frac{\partial^2\Phi_{1,2}(z)}{\partial z^2} = \left(\gamma - f_1 k_\perp^2\right)\Phi_{1,2}(z), \qquad (4)$$

If one chooses the origin of z -axis in the middle of two-dimensional layer with thickness d than the hard wall boundary conditions take the following form: $\Phi(\pm d/2)=0$, so, in this approximation taking into account (4) we obtain:

$$\begin{cases}\Phi_{pn}(z)=\cos(k_n z)\ (n=1,3,5\ldots)\ \text{for p}=1\\ \Phi_{pn}(z)=\sin(k_n z)\ (n=2,4,6\ldots)\ \text{for p}=-1\end{cases}, \qquad (5)$$

where $\mathrm{p}=\pm 1$ is a parity, $k_n=\pi n/d$, and

$$\gamma(\varepsilon)=f_1(\varepsilon)k_\perp^2+f_2(\varepsilon)k_n^2. \qquad (6)$$

The dispersion equation (6) describes four sets of subbands with different numbers n. Each subband is twofold degenerated for the arbitrary value of $k_\perp$. These are: conduction subbands (c), heavy-hole valence subbands ($j=1$), light-hole valence subbands ($j=2$) and spin-orbit split-off valence subbands ($j=3$). Here index j enumerates sets of valence subbands in decreasing order of their energies. The independence of energy spectrum from the direction of $\mathbf{k}_\perp$ is the consequence of coinciding of main crystalline axis with the normal to the two-dimensional layer's plane.

Because of F_1 independence from F_2 we have two independent orthogonal functions $\mathbf{\Psi}_\sigma(\mathbf{r})$, which we enumerate by index $\sigma=1,2$. The rest of functions $F_3\ldots F_8$ can be found using (3), (5) in terms of F_σ as $F_{i\sigma}=c_{i\sigma}F_\sigma$, where the coefficients $c_{i\sigma}$ listed in Table 1.

Therefore, in our case the wave function of electron

Table 1 – The coefficients $c_{i\sigma}$

Coefficient	$\sigma=1$	$\sigma=2$
$c_{3\sigma}$	$-\dfrac{\mathrm{p}Pk_n}{(\varepsilon+2\Delta/3)}\hat{\mathrm{P}}$	$-\dfrac{iPk_-}{(\varepsilon-\varepsilon_g)}$
$c_{4\sigma}$	$\dfrac{iPk_+}{(\varepsilon-\varepsilon_g)}$	$-\dfrac{\mathrm{p}Pk_n}{(\varepsilon+2\Delta/3)}\hat{\mathrm{P}}$
$c_{5\sigma}$	$-\dfrac{\mathrm{p}Pk_n}{(\varepsilon-\varepsilon_g)}\hat{\mathrm{P}}$	$-\dfrac{iPk_-}{(\varepsilon+\delta+\Delta/3)}$
$c_{6\sigma}$	0	$-\dfrac{\mathrm{p}Pk_n}{(\varepsilon-\varepsilon_g)}\hat{\mathrm{P}}$
$c_{7\sigma}$	0	$-\dfrac{iPk_+}{\varepsilon}$
$c_{8\sigma}$	$\dfrac{-iPk_-}{\varepsilon}$	0

Note: $\hat{\mathrm{P}}$ is the operator that changes sign of the $\varphi_{pn}(z)$ parity.

At fixed value of modulus $k_\perp$ depends on type of subband (c or j), quantum numbers σ, p, n and the value of polar angle $\varphi=\arctan\left(k_y/k_x\right)$.

Taking into account the relations

$$\langle u_i|u_{i'}\rangle=\delta_{ii'},\quad \int_{-d/2}^{d/2}\Phi_{pn}(z)\Phi_{p'n'}(z)dz=(d/2)\delta_{pp'}\delta_{nn'},$$

(here u_i is the Bloch amplitude, δ_{ij} is the Kronecker symbol) and considering that envelope functions vary slightly under the crystal volume V one gets:

$$\frac{1}{N}\sum_N\int_V F_{i\sigma}^* u_i^* F_{i'\sigma}u_{i'}dV=\frac{1}{V}|A_\sigma|^2|c_{i\sigma}|^2\overline{\Phi_i^2(z)}V\delta_{ii'}=\frac{1}{d}|A_\sigma|^2|c_{i\sigma}|^2\int_{-d/2}^{d/2}\Phi_i^2(z)dz\delta_{ii'}=\frac{1}{2}|A_\sigma|^2|c_{i\sigma}|^2\delta_{ii'}. \qquad (7)$$

(here we applied the first mean value theorem for integration). Without loss of generality we assume that $|A_\sigma|_{\sigma=1}^2=|A_\sigma|_{\sigma=2}^2=|A|^2$ and using expression (7) and normalization condition $\langle\mathbf{\Psi}_\sigma|\mathbf{\Psi}_\sigma\rangle_{\sigma=1}+\langle\mathbf{\Psi}_\sigma|\mathbf{\Psi}_\sigma\rangle_{\sigma=2}=1$ we derive

$$|A|^2=\left[1+\frac{P^2k_\perp^2}{2}\left(\frac{1}{(\varepsilon-\varepsilon_g)^2}+\frac{1}{\left(\varepsilon+\delta+\frac{1}{3}\Delta\right)^2}+\frac{1}{\varepsilon^2}\right)+P^2k_n^2\left(\frac{1}{\varepsilon+\varepsilon_g^2}+\frac{1}{\left(\varepsilon+\frac{2}{3}\Delta\right)^2}\right)\right]^{-1}. \qquad (7)$$

The knowledge of energy subband structure and wave functions allows deriving the expression for imaginary part of dielectric function $\varepsilon_{\mathrm{i}}(\omega)$ that is responsible for the optical absorption in crystals. According to [9] in the case of direct optical transitions the general formula for it has the following form:

$$\varepsilon_{\mathrm{i}}(\omega)=\frac{\pi e^2}{\varepsilon_0 m_0^2\omega^2 V}\sum_{\mathrm{n,m}}\left|\langle\mathrm{n}|(\mathbf{u},\hat{\mathbf{p}})|\mathrm{m}\rangle\right|^2\left(f(\varepsilon_{\mathrm{m}})-f(\varepsilon_{\mathrm{n}})\right)\delta\left(\varepsilon_{\mathrm{n}}-\varepsilon_{\mathrm{m}}-\hbar\omega\right)\delta_{\mathbf{k}_\perp\mathbf{k}'_\perp},. \qquad (8)$$

where $\mathbf{u}$ is the polarization vector of electromagnetic wave; $\hat{\mathbf{p}}=-i\hbar\nabla$ is the momentum operator; $f(\varepsilon)$ is the Fermi function; $\delta\left(\varepsilon_{\mathrm{n}}-\varepsilon_{\mathrm{m}}-\hbar\omega\right)$ is the delta function. The summation in (8) is taking over all states for which the following conditions are executed: $\mathbf{k}_\perp=\mathbf{k}'_\perp$, where ε_{m}, $\mathbf{k}_\perp$ are respectively initial energy and wave vector of electron; ε_{n}, $\mathbf{k}'_\perp$ are the energy and wave vector of excited electron. It should be noted that as-grown samples of Cd_3As_2 are degenerate n-type semiconductors. However, the extreme electrostatic charge doping in single-crystalline thin films of this compound enables significantly lower the position of Fermi level up to

change in the type of conductivity [11]. That is why in the following below we assume that all states of the valence subbands are fully occupied while all conduction subbands are empty so the bracket $f(\varepsilon_{\rm m})-f(\varepsilon_{\rm n})$ is equal to 1. In the case of Cd_3As_2 such a condition can be realized if the Fermi level corresponds to zero energy and the absolute temperature $T=0$.

Since the allowed values of vector $\mathbf{k}_\perp$ fill the reciprocal plane with density of $V/(4\pi^2 d)$ one can obtain from (8):

$$\varepsilon_{\rm i}(\omega)=\frac{e^2}{4\pi^2{}_0 m_0^2\omega^2 d}\sum_j\sum_{\sigma_c,\sigma_j}\sum_{p_c,p_j}\sum_{n_c,n_j}\int_0^\infty k_\perp dk_\perp\int_0^{2\pi}\left|\left\langle\mathbf{\Psi}_{c\sigma_c p_c n_c}(k_\perp)\left|\mathbf{u}\hat{\mathbf{p}}\right|\mathbf{\Psi}_{j\sigma_j p_j n_j}(k_\perp)\right\rangle\right|^2\delta(\varepsilon_{cn_c}-\varepsilon_{jn_j}-\hbar\omega)d\varphi\,. \quad (9)$$

In finding the optical matrix element $\left\langle\mathbf{\Psi}_{c\sigma_c p_c n_c}\left|\mathbf{u}\hat{\mathbf{p}}\right|\mathbf{\Psi}_{j\sigma_j p_j n_j}\right\rangle$ we took into account smoothness of spatial variation of envelope functions as compared to Bloch amplitudes and consider them as constants, while taking partial derivatives of the product $F_{i'\sigma}u_{i'}$. Also we applied the technique of calculating of volumetric integral as it was done in the derivation of formula (7) and considered that the selection rules in quasi-cubic model are as follows: $\langle S|\hat{p}_x|X\rangle=\langle S|\hat{p}_y|Y\rangle=\langle S|\hat{p}_z|Z\rangle=(im_0/\hbar)P$ (all the other types of matrix elements are equal to zero). As a result we obtained:

$$\sum_{\sigma_c,\sigma_j}\sum_{p_c,p_j}\sum_{n_c,n_j}\int_0^{2\pi}\left|\left\langle\mathbf{\Psi}_{c\sigma_c p_c n_c}(k_\perp)\left|\mathbf{u}\hat{\mathbf{p}}\right|\mathbf{\Psi}_{j\sigma_j p_j n_j}(k_\perp)\right\rangle\right|^2 d\varphi=\sum_n\frac{\pi m_0^2P^4k_\perp^2}{4\hbar^2}\left|A_{cn}\right|^2(k_\perp)\left|A_{jn}\right|^2(k_\perp)M_{\mathbf{u}cjn}(k_\perp)\,,$$

where for the transversal plane polarization of light $\mathbf{u}\perp z$ $(\mathbf{u}=\mathbf{u}_\perp)$

$$M_{\mathbf{u}_\perp cjn}=\left(F_1(\varepsilon_{cn})+F_1(\varepsilon_{jn})\right)^2+\left(F_2(\varepsilon_{cn})-F_2(\varepsilon_{jn})\right)^2, \quad (10)$$

in the longitudinal polarization $\mathbf{u}\parallel z$ $(\mathbf{u}=\mathbf{u}_\parallel)$

$$M_{\mathbf{u}_\parallel cjn}=F_3^2(\varepsilon_{cn})+F_3^2(\varepsilon_{jn})\,, \quad (11)$$

The following notations are introduced in the formulas (10-11):

$$F_1(\varepsilon)=\frac{\varepsilon\left(\varepsilon+\frac{2}{3}\Delta\right)+\delta\left(\varepsilon+\frac{1}{3}\Delta\right)}{\varepsilon\left(\varepsilon\left(\varepsilon+\Delta\right)+\delta\left(\varepsilon+\frac{2}{3}\Delta\right)\right)},$$

$$F_2(\varepsilon)=\frac{\Delta(\varepsilon+\delta)}{3\varepsilon\left(\varepsilon\left(\varepsilon+\Delta\right)+\delta\left(\varepsilon+\frac{2}{3}\Delta\right)\right)},$$

$$F_3(\varepsilon)=\frac{\Delta}{3\left(\varepsilon\left(\varepsilon+\Delta\right)+\delta\left(\varepsilon+\frac{2}{3}\Delta\right)\right)},$$

Therefore, in the approximation used the only transitions with $n_j=n_c$ are allowed.

To execute integration over $k_\perp$ in (9) one may use properties of the delta function. It is well known that

$$\int_{x_1}^{x_2}g(x)\delta\left(f(x)\right)dx=\sum_{x_0}g(x_0)\left|\frac{df}{dx}\right|^{-1}_{x=x_0},$$

where we denoted zeros of $f(x)$ on the interval from x_1 to x_2 through x_0. In our case there may be (or may not be at all) only one value of $k_\perp$ at which direct optical transition exists for fixed photon energy $\varepsilon_{\rm ph}=\hbar\omega$ and pair of subbands. This value we denote as $k_{\perp cjn}$. Finally, we have

$$\varepsilon_{\rm i}(\varepsilon_{\rm ph})=\frac{e^2P^4}{16\varepsilon_0\varepsilon_{\rm ph}^2 d}\sum_j\sum_n\left\{k_\perp^3\left|A_{cn}\right|^2(k_\perp)\left|A_{jn}\right|^2(k_\perp)M_{\mathbf{u}cjn}(k_\perp)\left|\frac{\partial\varepsilon_{cn}(k_\perp)}{\partial k_\perp}-\frac{\partial\varepsilon_{jn}(k_\perp)}{\partial k_\perp}\right|^{-1}\right\}_{k_\perp=k_{\perp cjn}}. \quad (12)$$

3. NUMERICAL RESULTS AND DISCUSSION

As an example we consider the application of derived expressions to the computation of energy and absorption spectrum in QW based on Cd_3As_2. As the set of band parameters of this material we used [7]: $P=7.4\cdot10^{-10}$ eV·m, $\varepsilon_g=-0.1$ eV, $\Delta=0.3$ eV, $\delta=0.1$ eV. Fig. 2 a, b shows its energy subbands arrangement near $k_\perp=0$ for two cases: $d=50$ nm (a) and $d=10$ nm (b).

There are four set of subbands relevant to the optical absorption edge.

It is clearly seen that in both cases light-hole and split-off valence subbands "move" downward on the energy scale in a conventional manner with the increasing of number n.

For the two other type of subbands the situation is more complex. In the first case the energy of $n=1$ heavy-hole valence subband $\varepsilon_{11}(0)<0$ and the bottom of appropriate conduction subband corresponds to the energy $\varepsilon=0$ at $k_\perp=0$. With increasing of number n the energy ε_{1n}, while staying negative at $k_\perp=0$, increases, whereas the bottom of appropriate conduction subband corresponds to the energy $\varepsilon=0$ at $k_\perp=0$. Such a pattern exists up to a certain number n_0 (for $d=50$ nm $n_0=3$) beginning from which top of each heavy-hole valence subband corresponds to the energy

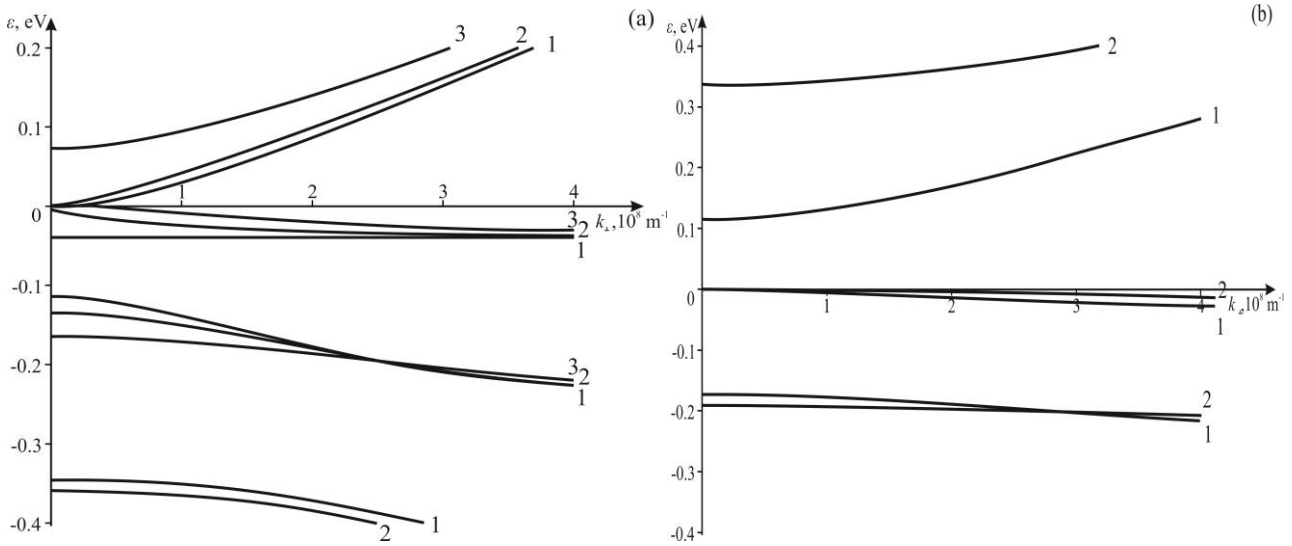

Fig. 2 – The dependencies $\varepsilon(k_\perp)$ for the four sets of subbands $k_\perp = 0$. The numbers 1, 2, 3 correspond to the values of the quantum number n. (a) – $d = 50\,\text{nm}$; (b) – $d = 10\,\text{nm}$

$\varepsilon = 0$ at $k_\perp = 0$. At the same time bottom of appropriate conduction subband corresponds to the increasing with rising of number n energy $\varepsilon > 0$ at $k_\perp = 0$. The transition from the first to the second case should take place at critical value of d: $d_{\text{cr}} = \pi P \Big/ \sqrt{-\varepsilon_g \delta} \approx 23\,\text{nm}$ (this relation can be easily obtained from equation (6) if one puts in it $n = 1$, $k_\perp = 0$, $\varepsilon = 0$).

Let us now consider the peculiarities of interband absorption within the frameworks of derived expression (14). First of all, we note that the effective optical energy gap ε_g^* in QW based on Cd_3As_2 should vary in non-trivial way with the changing of thickness d, when $d > d_{\text{cr}}$ (see Fig 3 a). This circumstance is caused by the anomalies discussed above in the position of the first few conduction and heavy-hole valence subbands. More exactly, such a modulation is periodic in d. The nodes d_n of such "damped oscillations" can be easily obtained from the equation $(\gamma(\varepsilon)/f_2(\varepsilon))_{\varepsilon=0} = k_n$: $d_n = n d_{\text{cr}}$ Therefore, the oscillations period is also equal to d_{cr}. With $d_n < d_{\text{cr}}$ ε_g^* increases in usual manner, when thickness of QW is decreasing. We can call this effect "blue shift delay" or "deferred blue shift".

The peculiarity $\varepsilon_g^*(d)$ of Cd_3As_2 considered above was earlier reported in [12] within the framework of model, which includes second order perturbation theory, but neglects spin-orbit splitting of valence band and nonparabolicity of bands as it is in our case. Here we present more comprehensive analysis based on the energy spectrum of QW for arbitrary orientation of quantum confinement to the main crystalline z-axis calculated below. Let us introduce the axis transformation

$$\begin{cases} x' = \cos\theta_0 x - \sin\theta_0 z \\ y' = y \\ z' = \sin\theta_0 x + \cos\theta_0 z \end{cases},$$

where θ_0 is the angle between the main crystalline z-axis and the normal to the two-dimensional layer plane. In the new coordinate system the equation (2) takes the following form:

$$\left(\gamma(\varepsilon) + \left[f_1(\varepsilon)\cos^2\theta_0 + f_2(\varepsilon)\sin^2\theta_0 \right] \frac{\partial^2}{\partial x'^2} + f_1(\varepsilon)\frac{\partial^2}{\partial y'^2} + \left[f_1(\varepsilon)\sin^2\theta_0 + f_2(\varepsilon)\cos^2\theta_0 \right] \frac{\partial^2}{\partial z'^2} + \right.$$
$$\left. + \left[f_1(\varepsilon) - f_2(\varepsilon) \right] \sin 2\theta_0 \frac{\partial^2}{\partial x' \partial z'} \right) F = 0. \qquad (13)$$

The substitution $F = A\exp\left[i(k_x' x' + k_y' y') \right] \Phi(z')$ into this equation leads us to the following ordinary differential equation:

$$\left(\frac{\partial^2}{\partial z'^2} + ia\frac{\partial}{\partial z'} + b \right) \Phi(z') = 0,$$

where

$$a = \frac{\left[(f_1(\varepsilon) - f_2(\varepsilon)) \sin 2\theta_0 \right] k_\perp \cos\varphi}{f_1(\varepsilon)\sin^2\theta_0 + f_2(\varepsilon)\cos^2\theta_0}, \quad b = \frac{\gamma(\varepsilon) - \left[(f_1(\varepsilon)\cos^2\theta_0 + f_2(\varepsilon)\sin^2\theta_0)\cos^2\varphi + f_1(\varepsilon)\sin^2\varphi \right] k_\perp'^2}{f_1(\varepsilon)\sin^2\theta_0 + f_2(\varepsilon)\cos^2\theta_0},$$

and $k'_\perp = \sqrt{k'^2_x + k'^2_y}$, $\varphi = \arctan(k'_y/k'_x)$. The solution of the equation (13) in hard wall approximations has form:

$$\begin{cases} \Phi_{pn}(z') = \exp(-idz'/2)\cos(k_n z') \ (n = 1,3,5\ldots) \text{ for p} = 1 \\ \Phi_{pn}(z') = \exp(-idz'/2)\sin(k_n z') \ (n = 2,4,6\ldots) \text{ for p} = -1 \end{cases},$$

where p=±1 is a parity, $k_n = \pi n/d$, and

$$\gamma(\varepsilon) = f_1(\varepsilon)\left[\sin^2\varphi + \cos^2\varphi \frac{f_2(\varepsilon)}{f_1(\varepsilon)\sin^2\theta_0 + f_2(\varepsilon)\cos^2\theta_0}\right]k'^2_\perp + \left[f_1(\varepsilon)\sin^2\theta_0 + f_2(\varepsilon)\cos^2\theta_0\right]k_n^2. \quad (14)$$

Therefore, with $\theta_0 \neq 0$ the energy spectrum is anisotropic in the reciprocal plane. It should be noted that with $k'_\perp \neq 0$ there are two extra spurious solutions [13] of the equation (14) so, one has to take into account only that four solutions, which occur with $k'_\perp = 0$.

Due to the condition

$$\int_{-d/2}^{d/2} \Phi_{pn}(z)\Phi_{p'n'}(z)dz = (d/2)\delta_{pp'}\delta_{nn'}$$

for all angles of θ_0 the only transitions with $\Delta n = 0$ are allowed. The extremum of each energy subband is located at $k'_\perp = 0$, so the equations for finding energy levels, between which direct optical transition take place from (2B), has following form:

$$\gamma(\varepsilon) = \left[f_1(\varepsilon)\sin^2\theta_0 + f_2(\varepsilon)\cos^2\theta_0\right]k_n^2. \quad (15)$$

In Fig. 3 b-d there are shown theoretical dependences $\varepsilon_g^*(d)$ for different angles θ_0 between the main crystalline z-axis and the normal to the two-dimensional layer's plane calculated with the help of numerical solutions of the equation (15). The following patterns are clearly seen:

1. The considered behavior $\varepsilon_g^*(d)$ takes place with $\theta_0 \neq 0$;

2. The oscillations period rapidly increases with rising of θ_0, reaching the value of 132 nm at $\theta_0 = 90^\circ$;

3. The ε_g^* value, which corresponds to the minima of oscillations, becomes non-zero with $\theta_0 \neq 0$ this value, however, is very small (< 60 meV);

4. The magnitude of oscillations rapidly decreases with θ_0 rising.

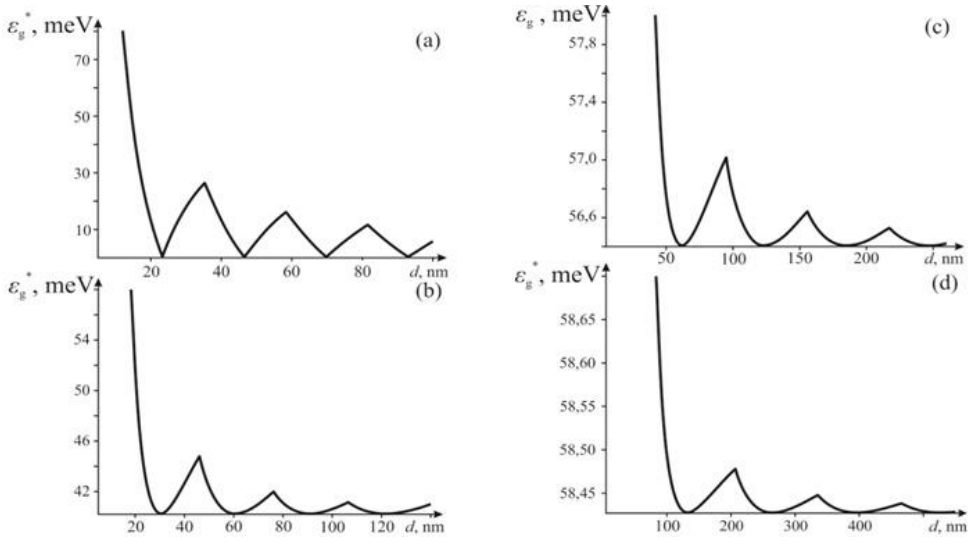

Fig. 3 – The dependencies $\varepsilon_g^*(d)$ for different angles θ_0: a) $\theta_0 = 0^\circ$; b) $\theta_0 = 30^\circ$; c) $\theta_0 = 60^\circ$; d) $\theta_0 = 90^\circ$

The considered peculiarities of $\varepsilon_g^*(d,\theta_0)$ dependence may be fully explained by the structure of heavy-hole valence band in the vicinity of Γ-point. Due to presence of "dent" in it, the energy level of each $j=1$ subband with $k=1$ "moves" upward on the energy scale from the start of QW thickness decreasing. However,

this speed of "moving" is greater than the speed of conduction subband energy level "raising" with the same number of n on a certain interval of d changing. Because of this fact the energy gap, which is defined by the pair of the nearest conduction and heavy-hole energy levels with the same number of n, initially decreases and then begins to increase. Such an increasing further is replaced by the decreasing of ε_g^* caused by the mutual arrangement of $n' = n-1$ pair.

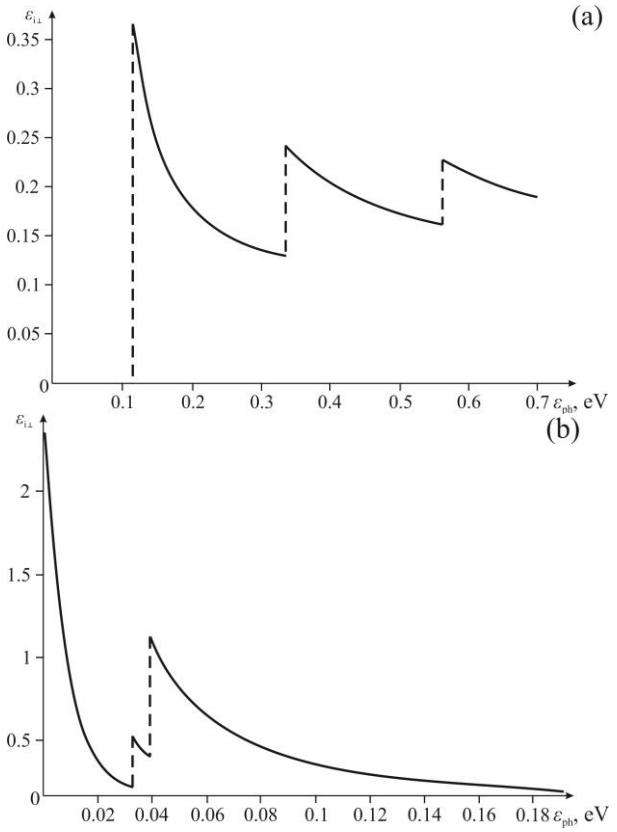

Fig. 4 – The dependencies $\varepsilon_{i\perp}(\varepsilon_{ph})$ for the following thicknesses of a two-dimensional layer: (a) – $d = 50\,\text{nm}$; (b) – $d = 10\,\text{nm}$

In Fig. 4 a, b there are presented results of numerical calculations of $\varepsilon_i(\varepsilon_{ph})$ dependence in the case of transversal light polarization for the following thicknesses of QW: $d = 50\,\text{nm}$ (a) and $d = 10\,\text{nm}$ (b). The analysis of resulted curves shows that the transitions between heavy-hole and conduction subbands make absolutely predominant contribution to the optical absorption in infrared region. The interband absorption caused by the transitions from the light-hole and spin-orbit split-off valence subbands is comparatively too weak to be neglected. The considered peculiarity comes from the fact that heavy-hole subbands energies of electrons that take part in the direct interband transitions are too close to zero. For the same reason the absorption for longitudinal light polarization many orders of magnitude smaller than for transverse because the heavy-hole subbands energies of electrons that take part in the direct interband transitions are too close to zero (see expressions (10), (11)).

4. CONCLUSIONS

In the presented paper we developed the theory of optical absorption in rectangular QWs with infinite barriers based on bulk materials with anisotropic non-parabolic bands. We used quasi-cubic approximation in eight-band Kane model and derived both wave functions and the dispersion equation for finding electronic energy spectrum for such structures. Using these results we obtained the expression for imaginary part of dielectric function in the case of direct interband optical transitions.

Further, we applied our theory for the numerical calculations of optical energy gap and interband absorption for Cd_3As_2 QW at its different thicknesses and orientation of quantum confinement to the main crystalline axis.

It was shown that due to the Dirac-type of this material several peculiarities should appear. These are energy gap oscillation and "blue shift delay".

Теорія міжзонного оптичного поглинання в квантових ямах на основі об'ємних матеріалів з анізотропними непараболічними зонами

В.В. Івченко[1], В.С. Щербюк[2]

[1] *Херсонська державна морська академія, просп. Ушакова, 20, 73000 Херсон, Україна*
[2] *Херсонський державний університет, вул. Університетська, 27, 73000 Херсон, Україна*

Розвинуто теорію іж зонного оптичного поглинання в прямокутних квантових ямах з нескінченними бар'єрами, що базуються на матеріалах з сильно непараболічним анізотропним енергетичним спектром електронів. Числові розрахунки виконано для тривимірного діраківського напівметала – арсеніду кадмію. Особливу увагу приділено дослідженню ефектів осциляції ширини забороненої зони та «запізненню блакитного зсуву» в цьому матеріалі.

Ключові слова: Міжзонне оптичне поглинання, Квантова яма, Арсенід кадмію, Осциляції ширини забороненої зони, «Запізнювання блакитного зсуву».

Теория межзонного оптического поглощения в квантовых ямах на основе объемных материалов с анизотропными непараболическими зонами

В.В. Ивченко[1], В.С. Щербюк[2]

[1] *Херсонская государственная морская академия, просп. Ушакова, 20, 73000 Херсон, Украина*
[2] *Херсонский государственный университет, ул. Университетская, 27, 73000 Херсон, Украина*

Развита теория межзонного оптического поглощения в прямоугольных квантовых ямах с бесконечными барьерами, базирующимися на материалах с сильно непараболическим анизотропным спектром электронов. Численные расчеты выполнены для трехмерного дираковского полуметалла – арсенида кадмия. Особенное внимание уделено исследованию эффектов осцилляции ширины запрещенной зоны и «запаздыванию голубого сдвига» в этом материале.

Ключевые слова: Межзонное оптическое поглощение, Квантовая яма, Арсенид кадмия, Осцилляции ширины запрещенной зоны, “Запаздывание голубого сдвига”.

REFERENCES

1. M. Helm, *Intersubband Transitions in Quantum Wells: Physics and Device Applications* I, *Semiconductors and Semimetals* Vol. 62, chapter 1 (Academic Press, 2000).
2. W. Liu, D.H. Zhang, W. J. Fan, *Opt. Quantum Electronics* **38** No 12, 1101 (2006).
3. Г.Г. Зегря, Н.Л. Баженов, А.В. Шиляев, К.Д. Мынбаев, *Физ. Тех. Полупр.* **46** No 6, 792 (2012) (G.G. Zegrya, N.L. Bazhenov, A.V. Shilyayev, K.D. Mynbayev, *Semiconductors* **46** No 6, 773 (2012)).
4. L.C. Lew Yan Voon and M. Willatzen, The $k \cdot p$ *Method – Electronic Properties of Semiconductors* chapter 5.9.2 (Springer: 2009).
5. Z.K. Liu, J. Jiang, B. Zhou, Z.J. Wang, Y. Zhang, H.M. Weng, D. Prabhakaran, S.-K. Mo, H. Peng, P. Dudin, T. Kim, M. Hoesch, Z. Fang, X. Dai, Z.X. Shen, D.L. Feng, Z. Hussain, Y.L. Chen, *Nature materials* **13,** 677 (2014).
6. Q. Wang, C-Z. Li, S. Ge, J-G. Li, W. Lu, J. Lai, X. Liu, J. Ma , D-P. Yu, Z-M. Liao, D. Sun, *Nano Lett.* **17** No 2, 834 (2017).
7. В.В. Івченко, О.М. Сергеєв, В.С. Єльнік, Н.М. Чуйко, *ФХТТ* **4**(4), 673 (2003) (V.V. Ivchenko, O.M. Serheyev, V.S. Yelnik, N.M. Chuiko, *Phys. Chem. Solid State* **4**(4), 673 (2003)) [In Ukrainian].
8. Z. Wang, H. Weng, Q. Wu, Xi. Dai, Z. Fang, *Phys. Rev. B* **88** No 12, 125427 (2013).
9. T. Ihn, *Semiconductor Nanostructures*: *Quantum states and electronic transport*, chapter 4 (Oxford University Press: 2010).
10. V.V. Ivchenko, A.N. Sergeev, V.S. Elnik, G.P. Chuiko, *SPQEO* **8** No 2, 22 (2005).
11. Y. Liu, C. Zhang, X. Yuan, T. Lei, C. Wang, D. Di Sante, A. Narayan, L. He, S. Picozzi, S. Sanvito, R. Che, F. Xiu arXiv:1412.4380.
12. X. Xiao, S.A. Yang, Z. Liu, H. Li, G Zhou, arXiv:1408.2983v1.
13. B. Lassen, R.V.N. Melnik, M. Willatzen, *Commun. Comp. Phys.* **6** No 4, 699 (2009).